Geomechanics and Engineering, *Vol. 28, No. 2 (2022) 171-180*
https://doi.org/10.12989/gae.2022.28.2.171

Time-dependent compressibility characteristics of Montmorillonite Clay using EVPS Model

Moirangthem Johnson Singh[1a], Wei-Qiang Feng[2b], Dong-Sheng Xu[3c] and Lalit Borana[*1]

[1]*Discipline of Civil Engineering, Indian Institute of Technology Indore, India*
[2]*Department of Ocean Sciences and Engineering, The Southern University of Science and Technology, China*
[3]*School of Civil Engineering and Architecture, Wuhan University of Technology, China*

(Received February 16, 2021, Revised December 1, 2021, Accepted December 14, 2021)

Abstract. Time-dependent stress-strain behaviour significantly influences the compressibility characteristics of the clayey soil. In this paper, a series of oedometer tests were conducted in two loading patterns and investigated the time-dependent compressibility characteristics of Indian Montmorillonite Clay, also known as black cotton soil (BC) soil, during loading-unloading stages. The experimental data are analyzed using a new non-linear function of the Elasto-Visco-Plastic Model considering Swelling behaviour (EVPS model). From the experimental result, it is found that BC soil exhibits significant time-dependent behaviour during creep compared to the swelling stage. Pore water entrance restriction due to consolidated overburden pressure and decrease in cation hydrations are responsible factors. Apart from it, particle sliding is also evident during creep. The time-dependent parameters like strain limit, creep coefficient and $C_{\alpha e}/C_c$ are observed to be significant during the loading stage than the swelling stage. The relationship between creep coefficients and applied stresses is found to be non-linear. The creep coefficient increases significantly up to 630 kPa-760 kPa (during reloading), and beyond it, the creep coefficient decreases continuously. Several parameters like loading duration, the magnitude of applied stress, loading history, and loading path have also influenced secondary compressibility characteristics. The time-dependent compressibility characteristics of BC soil are presented and discussed in detail.

Keywords: black cotton soil; compressibility characteristics; creep and swelling; EVPS; oedometer

1. Introduction

Expansive soil is widely available geomaterials and natural resources for construction and infrastructure development projects. However, due to its intrinsic characteristics, these soils are problematic from the engineering perspective (Khademi and Budiman 2016). In India, the most expansive soil contains Montmorillonitic minerals along with illite and kaolinite (Gupta and Sharma 2016). These montmorillonite clays are also commonly referred to as Black cotton (BC) soil (Gidigasu and Gawu 2013). It covers about approximately *0.8* million square kilometres of geographic area, which is about *21.40%* of India's total geographical land area (Chandran *et al.* 2012). BC soil is predominantly found in western and central parts of India (Gupta and Sharma 2015). The clay containing montmorillonite possesses significant swelling due to adsorption of additional water between the combined structural sheets and continuous volumetric reduction under static loading, called consolidation. It is due to the combined effect of both the stress and time-dependent deformation. Both these effects continue simultaneously with the application of loads. The stress deformation is composed of hydrodynamic pore pressure dissipation and viscous deformation (Hawlader *et al.* 2003). Researchers have attempted to study the time-dependent stress-strain behaviour of the saturated expansive soil in both one-dimensional (Zhu 2017) and tri-axial strain conditions (Bjerrum 1967, Graham 1983). Different approaches have been proposed to capture the origin of the time-dependent deformation from these studies. Some of the factors responsible for time-dependent deformation are the viscous movement of adsorbing water around clay particles (Yin 2013), internal soil interaction, viscous arrangement and distortion of the clay particle arrangement and their skeleton structures (Mitchell and Soga 1993), particle sliding, delayed water that transfers and aggregates soil macro-pores (Mesri 1973, Navarro 2001).

The compression characteristics of a consolidated clay are generally linearized using a virgin consolidation line in e–log σ′ space, which interprets density hardening (Schofield and Wroth 1968, Terzaghi *et al.* 1996). Mesri and Godlewski (1977) suggested that there exists a unique relationship between the secondary compression index $C_{\alpha e}$ and compression index C_c. The relationship can also predict the volume change-logarithm of the time curve

∗Corresponding author, Assistant Professor
E-mail: lalitborana@gmail.com
[a]Doctoral student
E-mail: johnsonsingh124@gmail.com
[b]Assistant Professor
E-mail: fengweiqiang2015@gmail.com
[c]Professor
E-mail: dsxu@whut.edu.cn

ISSN: 2005-307X (Print), 2092-6219 (Online)

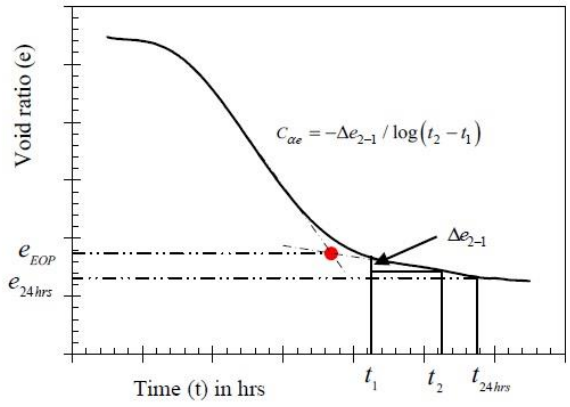

Fig. 1 Relationship between void ratio and logarithmic time

during the primary to secondary consolidation transition. Some researchers also studied this relationship for other soil types (Hawlader *et al*. 2003, Powell *et al.* 2012).

A semilogarithmic function $e = e_0 - (C_{\alpha e} \log t)$ has been used to study the creep strain behaviour of soft soil using Oedometric data, as shown in Fig. 1. Here e is the void ratio at any stage of loading, e_0 denotes the initial void ratio of the soil specimen, and $C_{\alpha e}$ indicates the coefficient of secondary consolidation and t is the duration of loading. But when loading duration tends to infinity, the void ratio e becomes negative. This concept is not acceptable and violates the physical law of mass existence (Yin 1999). Again, in the semilogarithmic function $\varepsilon_z = \varepsilon_{z0} + \left[C_c/(1+e_0)\right]\log\left(\sigma_z'/\sigma_{z0}'\right)$, where C_c = compression index; e_0 = void ratio corresponding to σ_{z0}'. Other stress-strain relationship is always invoked for the determination of volumetric strain. During the calculation of volumetric strain, a constant compressibility parameter is divided by arbitrary reference volume from which strain is supposed to be determined (Butterfield 1979). Again, when the applied stress σ_z' tends to infinity, the void ratio becomes negative. It meant that, as long as the stress has applied, the strain will continue, which is not possible; again, the void ratio of soil cannot be negative. It leads to a significant error in estimating the long-term settlement behaviour of soil. This concept is incorrect (Yin 2015). Apart from it, the function $\varepsilon_z = \varepsilon_{z0} + \frac{\psi^c}{V}\ln\left[\left(t_o^c + t_e^c\right)/t_o^c\right]$, where t_o^c is the time parameter, t_e^c is equivalent time related to creep, ψ^c/V is creep coefficient, ε_{z0} is the strain at a time $t = t_o^c$, leads to overestimates the creep considering long term (W. Feng *et al*. 2017, Singh *et al.* 2020). Several researchers highlighted the limitations of the conventional e–log σ′ framework in representing the non-linear compression behaviour of the natural clay soil (Butterfield 1979, Yuan and Whittle 2018). Since the study of delayed strain suggested by Bjerrum (1967), substantial efforts have been made to develop different models to examine the time-dependent behaviour of soft soils (Yin *et al.* 2002). Considering the viscous effect during the primary consolidation, several models were developed based on strain rate (Isotache model), the function of time (Hawlader *et al.* 2003). The isotache model assumes effective stress-strain behaviour, but this model cannot explain the relaxation behaviour (Yuan 2016). The strain rate model developed by Kabbaj *et al.* (1986) does not consider the viscous behaviour of clay prior to yield. Again, several constitutive models were developed by Leroueil *et al*. (1985) and Kelln *et al*. (2008) to describe the strain-rate-dependent stress-strain behaviour and the time-dependent behaviour of soft soil. But all these 1D and 3D models cannot consider both the time-dependent creep and swelling characteristics of soft soils (Yin and Tong 2011). Based on the function of time, Yin and Graham developed an EVP model to describe the time-dependent stress-strain behaviour of soils (Yin and Graham 1994, Yin 1990). Yin (1999) derived a non-linear function, which is a promising function to predict the time-dependent behaviour. Further, an attempt has been made to extend the model by considering the soil swelling behaviour (Feng *et al*. 2017).

From the literature, it is known that soft soil exhibits both creep and swelling behaviour, but there is limited information about the time-dependent strain during creep and swelling. Whether time-dependent strain during creep and swelling are the same or different at any instant or when time tends to infinity. Apart from it, the behaviour of the creep coefficient with the applied stress is not mentioned whether linear, non-linear, increases continuously or decrease continuously. This study aims to investigate the limitation discussed above and provide a reliable solution to better predict the long-term compressibility behaviour of expansive and problematic soils, such as the BC soil. To achieve this, a series of oedometer tests have been carried out at the Geotechnical Engineering laboratory of the Indian Institute of Technology Indore, using the BC soil in two different loading patterns. The results are examined under a variety of different loading and unloading stages. In this study, the EVPS Model is used due to advantages such as suitability for analyzing time-dependent behaviour (Nash 2001, Sun 1999). And it overcomes the drawbacks of other models by introducing model also introduces the limit timeline; if the equivalent time is set to be very large (infinity), the creep rate will be equal to zero (Yin 2015, Zdravkovic and Carter 2008).

2. The non-linear function of the EVPS model

For practicing engineers and academicians worldwide, the knowledge of better and reliable long term prediction models is of great importance to overcome overestimation or underestimation of the creep settlement. In this view, Yin (1999) proposed a function for fitting the non-linear creep behaviour of the expansive soil. The creep strain excluding the initial strain is given by

$$\varepsilon_z^c = \frac{\frac{\psi_0^c}{V}\ln\left(\frac{t_0^c + t_e^c}{t_0^c}\right)}{1 + \frac{\psi_0^c}{V\varepsilon_z^{cl}}\ln\left(\frac{t_0^c + t_e^c}{t_0^c}\right)} \quad (1)$$

where $\frac{\psi_0^c}{V}$, ε_z^{cl} and t_0^c are the constant parameters for specific stress applied. $\frac{\psi_0^c}{V}$ denotes the creep coefficient, ε_z^{cl} signifies the creep strain limit, and it is the distance between the reference timeline and creep equivalent limit (CEL) line (Yin and Tong 2011). When the time tends to infinity, $\varepsilon_z^c = \varepsilon_z^{cl}$ (Feng *et al.* 2017b, Yin 2015). If $\ln\left[\left(t_0^c + t_e^c\right)/t_0^c\right]$ is treated as a function *x*, the creep coefficient $\frac{\psi_0^c}{V} = a$ and the reciprocal of creep strain limit $1/\varepsilon_z^{cl} = b$, then the Eq. (1) can be expressed as

$$\frac{1}{\varepsilon_z^c}\ln\left(\frac{t_0^c + t_e^c}{t_0^c}\right) = \frac{1}{\varepsilon_z^{cl}}\ln\left(\frac{t_0^c + t_e^c}{t_0^c}\right) + \frac{V}{\psi_0^c} \tag{2}$$

The above equation is in the form of a straight line "y=bx+a" putting $\frac{1}{\varepsilon_z^c}\ln\left(\frac{t_0^c + t_e^c}{t_0^c}\right) = y$. The oedometer data were used to fit a straight line between the $\ln\left[\left(t_0^c + t_e^c\right)/t_0^c\right]$ against the $\ln\left[\left(t_0^c + t_e^c\right)/t_0^c\right]/\Delta\varepsilon_z^c$. The slope and intercept observed from this straight line were employed to determine the creep strain limit and creep coefficient, respectively.

The non-linear fitting curve function was further studied and extended, considering swelling behaviour (Feng *et al.* 2017). The swelling strain uses the non-linear function as follows

$$\varepsilon_z^s = -\frac{\frac{\psi_0^s}{V}\ln\left(\frac{t_0^s + t_e^s}{t_0^s}\right)}{1 + \frac{\psi_0^s}{V\varepsilon_z^{sl}}\ln\left(\frac{t_0^s + t_e^s}{t_0^s}\right)} \tag{3}$$

where $\frac{\psi_0^s}{V}$, ε_z^{sl} and t_0^s are the constant parameters for specific stress applied. $\frac{\psi_0^s}{V}$ denotes the creep coefficient, ε_z^{sl} signifies the creep strain limit, and it is the distance between the reference timeline and creep equivalent limit (CEL) line (Yin and Tong 2011). When the time tends to infinity, $\varepsilon_z^s = \varepsilon_z^{sl}$. If $\ln\left[\left(t_0^s + t_e^s\right)/t_0^s\right]$ is treated as a function x, the creep coefficient $\frac{\psi_0^s}{V} = a$ and the reciprocal of creep strain limit $1/\varepsilon_z^{sl} = b$, then the Eq. (3) can be expressed as

$$\frac{1}{\varepsilon_z^s}\ln\left(\frac{t_0^s + t_e^s}{t_0^s}\right) = -\frac{1}{\varepsilon_z^{sl}}\ln\left(\frac{t_0^s + t_e^s}{t_0^s}\right) + \frac{V}{\psi_0^s} \tag{4}$$

The above equation is in the form of a straight line "y=-bx+a" putting $\frac{1}{\varepsilon_z^s}\ln\left(\frac{t_0^s + t_e^s}{t_0^s}\right) = y$. The oedometer data were used to fit a straight line between the $\ln\left[\left(t_0^s + t_e^s\right)/t_0^s\right]$ against the $\ln\left[\left(t_0^s + t_e^s\right)/t_0^s\right]/\Delta\varepsilon_z^s$. The slope and intercept observed from this straight line were employed to determine the swell strain limit and swell coefficient, respectively. Using these functions, time-dependent compressibility characteristics of BC soil during loading-unloading stages will be discussed in the following sections.

3. Materials and testing procedures

This study used Black cotton soil to test 1D oedometer cells. The soil samples were collected from Indore region of Madhya Pradesh in India, from a depth of *1* m. The index properties of BC soil are obtained following the ASTM standards and are listed in Table 1. Fig. 2 depicts the particle size distribution curve of the BC soil.

The maximum dry density and optimum moisture content of the BC soil were determined using the standard Proctor equipment conform with ASTM D698-12. Before preparing the test specimen, the BC soil sample was kept in the oven at a temperature of *110* ± *5*℃ for *24* h. The oven-dried soil sample was exposed to the environment to attain room temperature. The factors like dry unit weight and initial moisture content constitutes a significant factor influencing the consolidation behaviour of expansive soil (Villar and Lloret 2008). So, BC soil was mixed with optimum moisture content and was compactedin a known volume in three different layers to attain maximum dry density (Kaniraj and Gayathri 2004). A *60* mm diameter with *20* mm height specimen was extracted from the compacted sample. The prepared sample was transferred to the steel ring and applied grease to reduce the possible friction between soil and the steel ring. The upper and lower surface of the prepared soil specimens were covered with

Table 1 Index properties of BC soil

Sl. No.	Parameters	Data
1.	Specific Gravity, G	2.720
2.	Liquid limit, w_l (%)	73.405
3.	Plastic limit, w_p (%)	34.120
4.	Plastic Index, I_p (%)	39.285
5.	Void Ratio, e_0	1.410
6.	Optimum moisture content (OMC)	27.020
7.	Maximum dry density, ρ_d (g/cm^3)	1.406

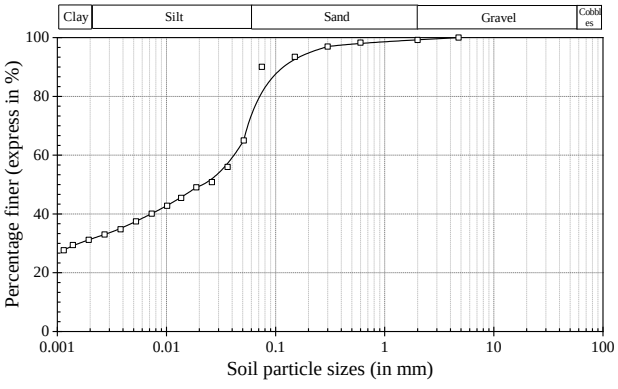

Fig. 2 Particle size distribution curve for BC soil

Table 2 Loading pattern arrangement for the oedometer (Singh *et al*. 2020)

Loading Pattern	Sl. No.	Loading (kPa)	Period (day)	Sl. No.	Loading (kPa)	Period (day)	Sl. No.	Loading (kPa)	Period (day)	Sl. No.	Loading (kPa)	Period (day)
	1	5	1	*11*	100	1	*21*	500	1	*31*	500	1
	2	10	7	*12*	250	1	*22*	1000	1	*32*	1000	1
	3	25	1	*13*	500	1	*23*	1250	7	*33*	1250	7
	4	50	1	*14*	1000	7	*24*	1000	1	*34*	1000	1
	5	100	7	*15*	500	1	*25*	500	1	*35*	500	1
E_1^*	*6*	50	1	*16*	250	1	*26*	250	1	*36*	250	1
	7	25	1	*17*	50	1	*27*	100	1	*37*	100	1
	8	10	7	*18*	10	7	*28*	10	7	*38*	50	1
	9	25	1	*19*	50	1	*29*	100	1	*39*	10	7
	10	50	1	*20*	250	1	*30*	250	1			
	1	5	7	*6*	250	7	*11*	10	7	*16*	1000	7
	2	10	7	*7*	500	7	*12*	50	7	*17*	1250	7
E_2^{**}	*3*	25	7	*8*	250	7	*13*	100	7			
	4	50	7	*9*	100	7	*14*	250	7			
	5	100	7	*10*	50	7	*15*	500	7			

Total days of loading is denoted as, * denotes 94 days, ** denotes 126 days

filter paper to resist the entrance of fine particles into the porous stones. The relative movement between the loading cap and base of the consolidation cell was recorded through a dial gauge clamped in the oedometer. A seating pressure of *5* kPa is applied for one day (ASTM Standard 2010; BS 1377, Part 5:1990). One dimensional multi-stage loading (MSL) oedometer tests were conducted on the prepared soil specimen. The whole experiment is performed at the normal room temperature of *25*±*2*°C. In the entire duration of loading and unloading, the soil sample was kept saturated Singh *et al.* (2020). Throughout the consolidation test, drainage was permitted from both the bottom as well as top of the test specimen. The load increment or decrement occurred after *24* h or more than *24* h to detect the proper consolidation curve. This loading pattern enables the soil to achieve the equilibrium of pore pressures. In this paper, the compressibility characteristics of BC soil is investigated by applying two different loading patterns E_1 and E_2 with varying intervals of time. The loading pattern and time of each specimen are interpreted in Table 2. Each loading pattern has its significance, (a) the load increment and decrement occurred every *24* h to reach a limiting load that applied for seven days. So E_1 was performed to analyze the effect of the unloading-reloading cycle on the swelling behaviour. (b) E_2 was performed to investigate the impact of loading time on swelling behaviour. All the load increments, as well as decrement, occurred every seven days. From both the loading pattern, it is known that each load is applied for a period in the range of *1* to *7* days. This particular arrangement is performed toprovide an equilibrium condition (Powell *et al.* 2012) and illustrate the long-term time-dependent characteristics of the soil (Yin 1999, Feng *et al.* 2017a).

4. Result from analysis and discussion

Fig. 3 illustrated the relationship between the change of vertical strain with time (log scale) during loading, unloading and reloading cycles in loading patternE_2. This vertical displacement consists of both primary and secondary consolidation. Compression in the primary consolidation stage is coupled with the dissipation of excess pore water from the interconnected voids of soil. The strain at which pore water pressure is negligible is called EOP. The time corresponding to this stage is called t_{eop} (Fatahi *et al*. 2013).

It is denoted by the graphical intersection of the tangent lines drawn between the two portions of strain against time. In this study, t_{eop} is assumed as t_0^c (Tan *et al.* 2018). According to the definition of the equivalent time and the reference timeline, the total strain at any point in the creep region or swelling region is considered to begin from the reference timeline (Yin and Graham 1994). This reference timeline is denoted by t_0^c and t_0^s during creep and swelling, respectively. At any time with respect to the reference timeline, the equivalent timeline can be calculated as, $t_e^c = t - t_0^c$, where t is the total duration of loading (Yin and Tong 2011). Using the above Eq. (2) and Eq. (4), various parameters during creep and swelling will be determined and discussed in the following sections. Singh *et al.* (2020) have studied comparison of two different functions in predicting the time-dependent creep and swelling behaviour of the BC soil EVPS model. So, particularly this non-linear function is used in this study for its accuracy and suitability in analyzing the BC soil.

In E_2, under the loading of *500* kPa, the analysis was performed and plotted the curve between the $\ln\left[\left(t_0^c + t_e^c\right)/t_0^c\right]/\Delta\varepsilon_z^c$ against $\ln\left[\left(t_0^c + t_e^c\right)/t_0^c\right]$ as shown in Fig. 4. Using the trend line, a straight line is plotted. The slope was obtained, and the intercept was converted to the corresponding parameters using Eq. (2). Thus, $\frac{\psi_0^c}{V}$ for the

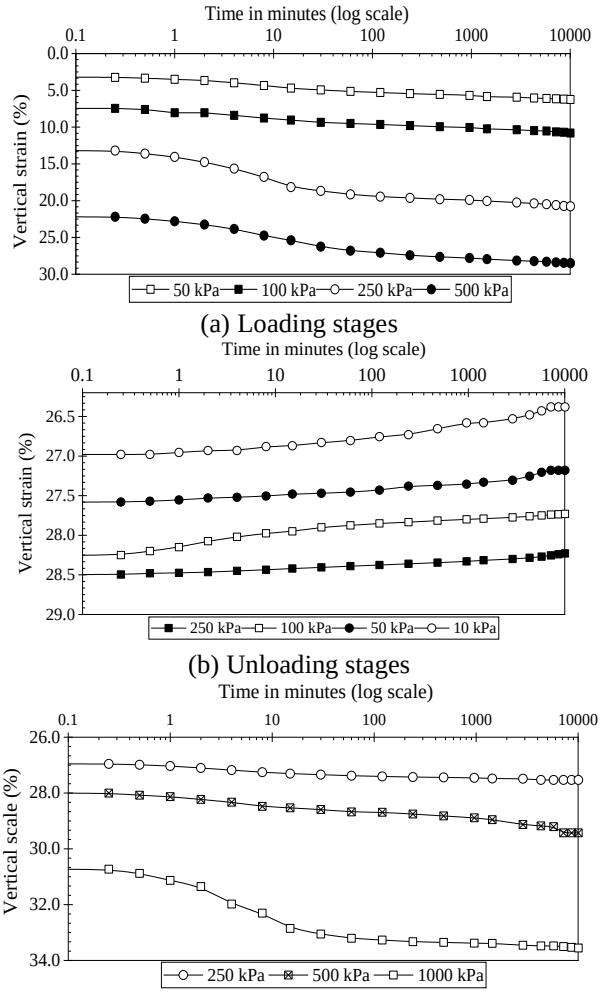

Fig. 3 Change in vertical strain with respect to time (express in log scale) for the sample specimen E_2

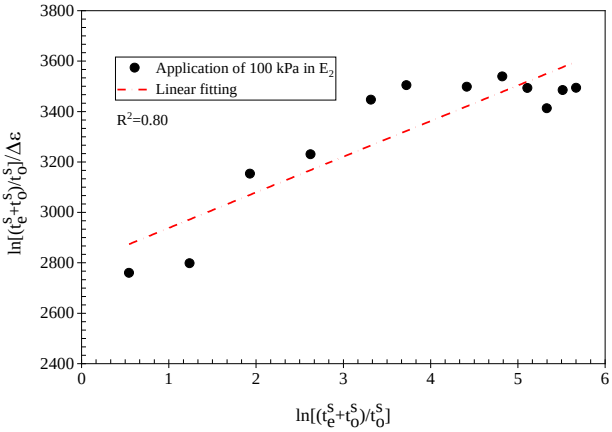

Fig. 5 Curve fitting parameters for Non-linear function during unloading of 100 kPa in E_2

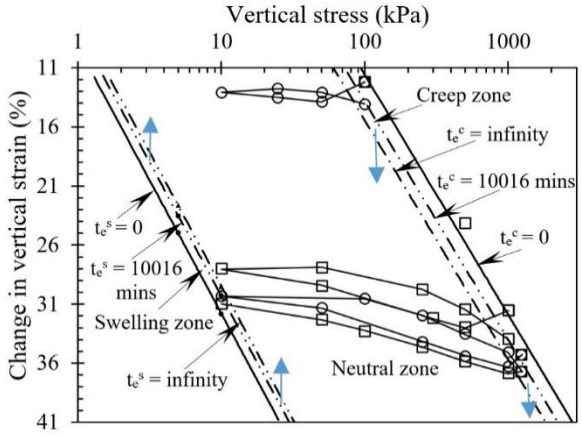

Fig. 6 Illustration of 1D creep and swelling strain in different equivalent time period using concept of EVPS Model for BC Soil (E_1)

BC soil is found to be *0.00781*, and the corresponding ε_z^{cl} is *0.0371*. Under the application of *500* kPa for an infinite period of time, the corresponding creep strain limit will be *0.0371*. The curve fitting parameter (R^2) value is more significant than *0.98*, and a good curve fitting is obtained with a non-linear creep function.

During the unloading of *100* kPa in E_2, all the parameters t_e^s, t_0^s were determined. Using the specified data, a curve was plotted in between $\ln\left[\left(t_0^s+t_e^s\right)/t_0^s\right]/\Delta\varepsilon_z^s$ against $\ln\left[\left(t_0^s+t_e^s\right)/t_0^s\right]$, as shown in Fig. 5. A straight line is plotted using the trend line. Using Eq. (4), the parameters $\frac{\psi_0^s}{V}$ for the BC soil is found to be *0.00031*, and the corresponding ε_z^{sl} is *0.01891*. This means that a maximum strain of *0.01891* will be recorded when the duration of unloading tends to be infinite for *100* kPa. The curve fitting parameter (R^2) value is found larger than *0.80*.

According to the EVPS model, under the application of a constant load, the time-dependent settlement of the specimen takes place in the creep region. Indistinguishably during the unloading, the specimen will undergo an expansion in the swell region. The final creep and swelling for infinite time are governed by an equilibrium line called Creep Equilibrium line (CEL) and Swelling Equilibrium line (SEL), respectively for creep and swelling. Between this CEL and SEL, the region is called a neutral zone where the soil is neither time-dependent creep nor swell. At any time, the strain can be derived using their equivalent timeline. In this study, at the equivalent time (t_e=*10016* mins), the strain for both creep and swelling are shown in Fig. 6.

Using EVPS Model, a comparison in time-dependent axial strain between creep and swelling is performed under effective stress *1250* kPa and 10 kPa, respectively. After reaching *1250* kPa, the strain at the equivalent time, $t_e = 0$ is *33.87%* strain. The effective stress *1250* kPa is remained applied for t_e=*10016* mins, the delayed strain changed into *36.4%* strain. After this, the loads are removed continuously till *10* kPa. After reaching *10* kPa, the strain at the equivalent time, $t_e = 0$ is *31.79%* strain. The effective stress *10* kPa is remained applied for t_e=*10016* mins, the delayed strain reached *30.3%* strain. Using the strain limit concept

in EVPS Model, the expected strain at $t_e \to \infty$ during the creep and swelling were determined and compared the data. Here at time t_e=*10016* mins, BC soil shows more significant strain during the creep stage than swelling. A similar pattern is observed when the time of loading as well as unloading tends to infinity. Creep deformation occurs due to the movement of pore water from microstructure (secondary structure) to macrostructure (primary structures) (Kaczmarek and Dobak 2017). However, during the swelling, the entrance of water occurs due to two significant reasons (Nelson 2016). Firstly, water enters due to completing the hydration shells of cation; this usually occurs in dried soil. But subsequent water enters by osmotic processes (Nelson *et al.* 2015). Due to pre-consolidated overburden, pressure restrains pore water flow through the interconnected voids. Thus the cation hydration between clay particles reduced subsequently. Therefore, the creep deformations were evident compared to swell. The strain after the EOP signifies the time-dependent behaviour of the geomaterials, and its slope can be computed through the secondary compression index $C_{\alpha e}$ (Feng *et al.* 2021). According to the EVPS model, the creep coefficient and secondary compression index are related as follows (Feng *et al*. 2017),

$$\frac{\psi_0^c}{V} = \ln(10)\frac{C_{\alpha e}}{V} = 2.3\frac{C_{\alpha e}}{V} \tag{5}$$

where *V* signifies the total volume occupied, $V = 1 + e_0$. To determine the creep and swelling behaviour parameters, the duration of loading and unloading should last as long as possible, respectively.

From the relationship between the void ratio and log time, significant changes in the void ratio are observed. This paper calculated the secondary compression index for each load increment in the reloading cycle using Eq. (5). The results are plotted between the calculated $C_{\alpha e}$ against normalized effective stress for E_1, as illustrated in Fig. 7 (a). The stress below the pre-consolidation pressure shows negligible void ratio changes with time. Appropriate points are not obtained to the plot after neglecting these stresses, so *5* kPa to *100* kPa for $E_1$are neglected here. So, in the first reloading phase, the stresses consider are *50* kPa-*100* kPa-*250* kPa-*500* kPa-*750* kPa-*1000* kPa, and the corresponding time-dependent component of compression $C_{\alpha e}$ are *0.00030, 0.00065, 0.00410, 0.00680, 0.00729* and *0.00634* respectively. A fitting curve was plotted, passing these points to find the maximum $C_{\alpha e}$ in the reloading cycle. The plotted trendline has an R^2 value of *0.99*. In the second reloading phase, *50* kPa-*250* kPa-*500* kPa-*1000* kPa the corresponding time-dependent component $C_{\alpha e}$ are respectively *0.00015, 0.00216, 0.00271* and *0.00204.* Similarly, in the third reloading cycle is composed of stress sequence *100* kPa-*250* kPa-*500* kPa-*1000* kPa-*1250* kPa and respective time-dependent component $C_{\alpha e}$ are *0.00041, 0.00155, 0.00215, 0.00190* and *0.00159*. The fitting curves were plotted for each 2nd and 3rd reloading cycle to the observed maximum $C_{\alpha e}$ for each reloading cycle. The R^2 values of the fitting curve are respectively *0.82* and *0.89*, which indicates small differences between the observed data and the fitted curve.

For each reloading stage, the $C_{\alpha e}$ is found to increase with the increase of effective stress. After reaching an optimum point, the time-dependent component $C_{\alpha e}$ is found to decrease as the void ratio cannot decrease indefinitely. A similar observation is noted in the case of Suzhou (SZ) soft soil, Tianjin (TJ) soil, Shanghai (SH) soft soil, as studied by Jiang *et al*. (2020). This stage is attributed to the more stable clay structure arrangement. This result shows that the void ratio will attain a limiting value with infinite loading time. The optimum $C_{\alpha e}$ during the first, second and third reloading cycle are respectively *0.00750, 0.00305* and *0.00234*, respectively. The second and third reloading cycle is reduced by *59.33%* and *68.80%*, respectively, regarding the first reloading cycle. The optimum time-dependent component $C_{\alpha e}$ is found reducing with the increase of the unloading-reloading cycle. The unloading-reloading cycle enhances the rearrangement of the soil particles. This cycle influences the two-level of the pore, i.e., intra-aggregate pores inside and between the clay particles and interaggregate pores between the clay aggregates (Nowamooz 2014, Shi *et al.* 2018). The soil particles undergo structuration to achieve a stable configuration during effective stress application. After completing the primary consolidation stage, pore water movement from the microstructure (secondary structure) to macrostructure (primary structures) occurs as the effective stress restrain continuously. This influences the sliding ability between particles. Once the pore inside the interaggregate and intra-aggregate particles vanishes, the creep coefficient shows declining. Beyond this, several other factors as mentioned above like adsorbing water around clay particles (Yin 2013), internal soil interaction, viscous arrangement and distortion of the clay particle arrangement and their skeleton structures (Mitchell and Soga 993), particle sliding, delayed water that transfers and aggregates soil macro-pores are responsible. Therefore, the creep coefficient shows decrement after attaining the maximum value. During the loading and reloading cycle, the skeleton structures and particle arrangement were destroyed continuously by water incursion and expulsion. Thus, the creep coefficient shows decrement against the loading and reloading cycles in the same applied stress. However, the soil attains its limiting creep coefficient in the stress range of *633.12* kPa-*757.97* kPa, irrespective of the number of loading-reloading cycles. The creep coefficient increase continuously and decrease after reaching the effective stress *633.12* kPa-*757.97* kPa. Thus there is a non-linear relationship between the creep coefficient and the applied stress.

Similarly, for the E_2, the stress below pre-consolidation pressure was neglected, so pressure sequence *5* kPa-*10* kPa *25* kPa are not considered. Fig. 7(b) shows the variation $C_{\alpha e}$ with different loading cycles for E_2. The sequence of effective stress applied consists of *50* kPa-*100* kPa-*250* kPa-*500* kPa and corresponding time-dependent parameter $C_{\alpha e}$ *0.00290, 0.00368, 0.00736* and *0.00518* respectively. The first reload sequence consist of *250* kPa-*500* kPa-*750* kPa-

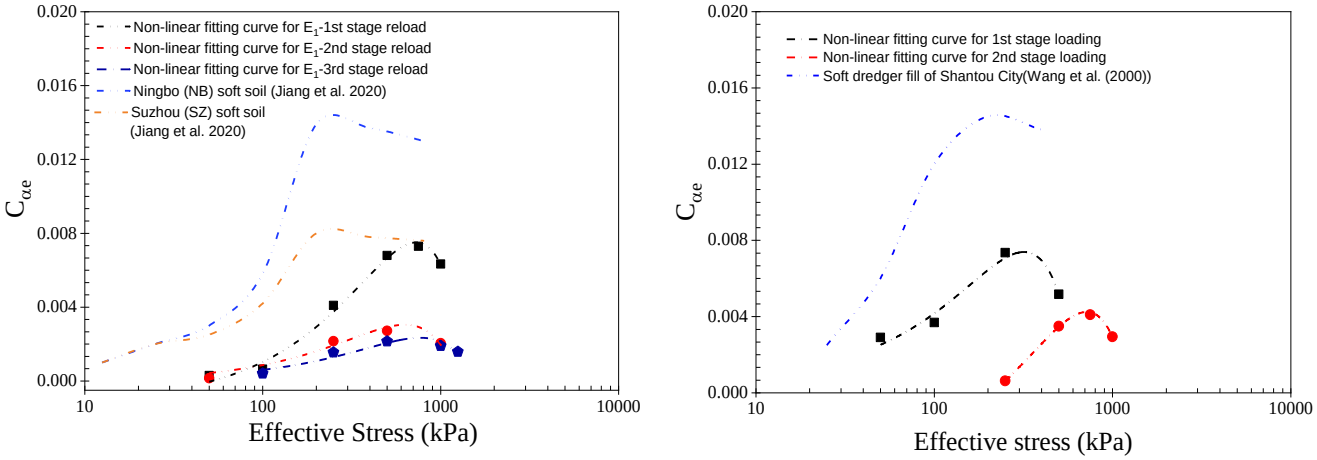

(a) E_1 loading pattern (b) E_2 loading pattern

Fig. 7 Relationship between $C_{\alpha e}$ and effective stress for each reloading cycle

1000 kPa, and their respective $C_{\alpha e}$ are *0.00063*, *0.00350*, *0.00411* and *0.00294*. A similar observation can be observed from the Soft dredger soil of Shantou City (Wang *et al.* 2020). Similarly, in the case of E2, the limiting creep coefficient is found in the range of 314.98 kPa and 718.55 kPa. The optimum time-dependent $C_{\alpha e}$ are *0.00740* and *0.00420*. The first reloading cycle is reduced by *43.24%*. The percentage comparison of reduction of E_2 is found decreasing with reference to E_1 *(59.33%>43.24%)*. This is because, in E_2, all the pressure is applied for *7* days continuously. This shows the duration of loading is an important factor influencing the time-dependent behaviour of soft soil. A higher loading period allows the soil to achieve an equilibrium of pore pressure. The result follows a consistency and is found similar to the study by other researchers (Suzanne Powell *et al.* 2012).

In E_2, there is a sudden shift of stress from *314.98* kPa to *718.55* kPa for achieving optimum time-dependent $C_{\alpha e}$. This is because the first cycle is the normal loading cycle, while the second is the reloading cycle, which influences the rearrangement of soil particles. From all these results, it is noted that the secondary compressibility behaviour is dependent on parameters like duration of loading, the magnitude of the applied stress, loading history, loading paths. Based on this parameter, Mesri classified the compressibility behaviour of different soil types, as shown in Table 3. Here it is known that BC soils belong to low to highly compressible soil. But in average value, the soil belongs to medium compressible soil, which is influenced by the plasticity of BC soil (Das 2019, Mesri 1973).

Table 3 Secondary compressibility behaviour as classified by Mesri (1973)

Sl. No.	Value ranges	Behaviour of secondary compressibility
1.	<0.002	Very low
2.	0.002-0.004	Low
3.	0.004-0.008	Medium
4.	0.008-0.016	High
5.	0.016-0.032	Very high

The ratio $C_{\alpha e}/C_c$ is consistent for a particular soil ranging from *0.025* for granular to *0.1* for peat soil. In this study, these parameters were derived from EVPS Model, and their relationship is compared with data derived by Mesri. The relationship C_c with void ratio and stress is shown below

$$\frac{C_c}{V}=\frac{\Delta\varepsilon_z}{\Delta\log\sigma'_z};\quad C_c=-\frac{\Delta e}{\Delta\log\sigma'_z} \tag{6}$$

where $\Delta\varepsilon_z=-\frac{e-e_0}{1+e_0}$ Similarly, for swelling behaviour

$$\frac{C_s}{V}=\frac{\Delta\varepsilon_z}{\Delta\log\sigma'_z};\quad C_s=-\frac{\Delta e}{\Delta\log\sigma'_z} \tag{7}$$

where $\Delta\varepsilon_z$ denotes the change in strain, $\Delta\log\sigma'_z$ signifies the change in the effective stress over one incremental load, V represents the volume $V=1+e_0$ and the initial void ratio. Using Eq. (7), the $C_{\alpha e}$ is derived from the non-linear function of EVPS model was plotted against C_c for BC soil, as shown in Fig. 8.

The $C_{\alpha e}/C_c$ during loading stage is found to be *0.0354*. It is almost consistent for the loading with an R^2 value of *92%*. The ratio of $C_{\alpha e}/C_c$ is varied with the difference of soil; for example, the ratio is observed *0.05* for San Francisco clay (Graham *et al.* 1983), *0.024* for Alban clay (Graham *et al.* 1983), *0.031* for Shanghai silty clay (Jiang *et al.* 2020) and *0.03* for Bearpaw Shale (Powell *et al.* 2012).

Similarly, Fig. 9 shows the ratio of $C_{\alpha e}/C_s$ during the swelling stage and is found to be *0.0299* with an R^2 value of

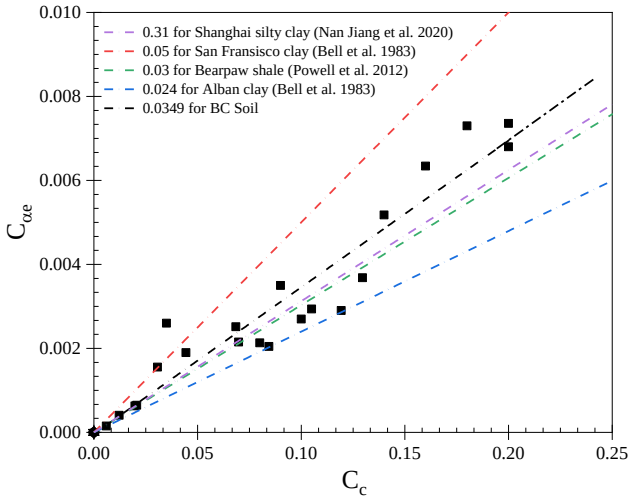

Fig. 8 Observe relationship between $C_{\alpha e}$ and C_c during load increments

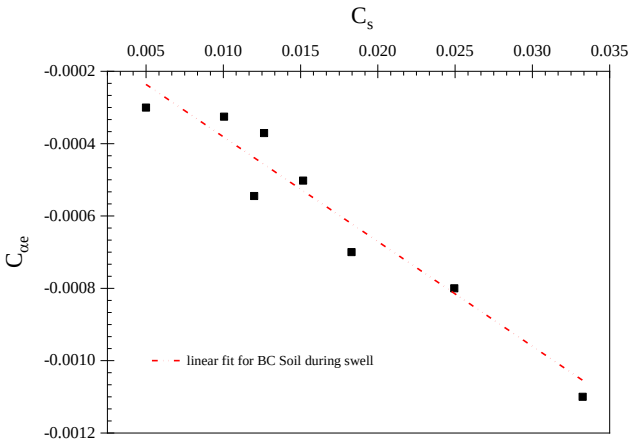

Fig. 9 Observe relationship between $C_{\alpha e}$ and C_s during unloading stages

83.76%. Using the non-linear function of the EVPS model, the ratio of $C_{\alpha e}/C_s$ for swelling behaviour of BC soil is reduced by *15.57%* as compared to the compression $C_{\alpha e}/C_c$. In representation, the ratio of $C_{\alpha e}/C_c$ is negative of the $C_{\alpha e}/C_s$. So, two ratios must be the same according to the relationship. But in the actual condition, the change of void ratio over time is not identical during creep and swelling stages. This might be influenced by several factors like consolidation pressure, sustained loads during loading and unloading stages (Mesri 1973). For example, in Fig. 3(a), there is a significant strain change during the application of *500* kPa. A similar pattern can be observed in preceding stress *250* kPa. But coming to Fig. 3(b), a significant change in strain can be observed in *10* kPa, and preceding stress *50* kPa. It is known that substantial strain can be observed in higher stress during loading stages, whereas smaller stress in unloading stages.

5. Conclusions

A series of one-dimensional MSL oedometer tests were conducted in Indian Montmorillonite Clay (BC) soil under different loading patterns to examine several time-dependent compressibility parameters like $\frac{\psi_0^c}{V}$, ε_z^{cl}, $\frac{\psi_0^s}{V}$, ε_z^{sl}, $C_{\alpha e}/C_s$, $C_{\alpha e}/C_c$. The experimental data were analyzed using EVPS Model. Based on the experimental study, the following conclusions are drawn;

- BC soil shows significant time-dependent behaviour/deformation during loading compared to the swelling stage. This is probably due to the influence of consolidated overburden pressure. It restrains the entrance of pore water through the interconnected voids and decreases cation hydration between clay particles during the unloading stage.
- The time-dependent creep coefficient $C_{\alpha e}$ increase continuously with the increase of effective stress. After reaching a maximum value (turning point), it reduces gradually. The turning point is found in the range of effective stress *630* kPa-*760* kPa (during reloading). This might be due to pore water movement from microstructure (secondary structure) to macrostructure (primary structures) after primary consolidation. This enhances the sliding ability between clay particles.
- The turning point is significantly influenced by the unloading-reloading cycle. With the increase of the unloading-reloading cycle, the parameter $C_{\alpha e}$ corresponding to a turning point decrease continuously and exhibits a non-linear relationship.
- Using the new function, the ratio of parameters $C_{\alpha e}/C_c$ for BC soil is found to be *0.0354*, which is almost found consistent as done by other researchers. Similarly, for the swelling behaviour, the ratio of $C_{\alpha e}/C_s$ for BC soil is *0.0299*, which is reduced by *15.57%* compared to $C_{\alpha e}/C_c$.
- Secondary compressibility behaviour is influenced by several factors like loading duration, applied stress, loading history, loading path.

References

Bjerrum, L. (1967), "Engineering geology of Norwegian normally-consolidated marine clays as related to settlements of building", *Geotechnique*, **17**(2), 81-118. https://doi.org/10.1680/geot.1967.17.2.83.

Butterfield, R. (1979), "A natural compression law for soils (an advance on e-log p')." *Géotechnique*, **29**(4). https://doi.org/10.1680/geot.1979.29.4.469.

Chandran, P., Ray, S., Mandal, C., Mandal, D., Prasad, J., Sarkar, D., Tiwary, P., Patil, N., Reddy, G.P.O., Lokhande, M., Wadhai, K., Dongare, V., Sidhu, G., Sahoo, A., Nair, K., Singh, S., Pal, D. and Bhattacharyya, T. (2012), "Revision of Black Soil Map of India for Sustainable Crop Production", *National Seminar on Geospatial Solutions for Resource Conservation and Management.*

Das, B.M. (2019), "Advanced soil mechanics", *Crc Press*.

Fatahi, B., Le, T.M., Le, M.Q. and Khabbaz, H. (2013), "Soil creep effects on ground lateral deformation and pore water pressure under embankments", *Geomech. Geoeng.*, **8**(2), 107-124. https://doi.org/10.1080/17486025.2012.727037.

Feng, W., Lalit, B., Yin, Z. and Yin, J.H. (2017a), "Long-term Non-linear creep and swelling behavior of Hong Kong marine

deposits in oedometer condition", *Comput. Geotech.*, **84**, 1-15. https://doi.org/10.1016/j.compgeo.2016.11.009.

Feng, W., Yin, J.H., Tao, X.M., Tong, F. and Chen, W.B. (2017b), "Time and strain-rate effects on viscous stress-strain behavior of plasticine material", *Int. J. Geomech.*, **17**(5). https://doi.org/10.1061/(ASCE)GM.1943-5622.0000806

Feng, R., Wang, L., Wei, K. and Zhao, J. (2021), "Consolidation settlement of soil foundations containing organic matters subjected to embankment load", *Geomech. Eng.*, **24**(1), 43-55. https://doi.org/10.12989/gae.2021.24.1.043.

Gidigasu, S.S.R. and Gawu, S.K.Y. (2013), "The mode of formation, nature and geotechnical characteristics of clack cotton soils-a review", *Standard Sci. Res. Essays*, **1(14)**, 377-390.

Graham, J., Crooks, J.H.A. and Bell, A.L. (1983), "Time effects on the stress-strain behaviour of natural soft clays", *Géotechnique*, **33**(3), 327-340. https://doi.org/10.1680/geot.1983.33.3.327.

Graham, J., Crooks, J.H.A. and Bell, A.L. (1983), "Time effects on the stress-strain behaviour of natural soft clays", *Géotechnique*, **33**(3), 327-340. https://doi.org/10.1680/geot.1983.33.3.327.

Gupta, C. and Sharma, R.K. (2015), "Study of black cotton soil and local clay soil for sub-grade characteristic", *Proceedings of the 50th Indian Geotechnical Conference*, 17th-19th December 2015, Pune, India.

Gupta, C. and Sharma, R.K. (2016), "Black cotton soil modification by the application of waste materials", *Periodica Polytechnica Civil Eng.*, **60**(4), 479-490. https://doi.org/10.3311/PPci.8010.

Hawlader, B.C., Muhunthan, B. and Imai, G. (2003), "Viscosity effects on one-dimensional consolidation of clay", *Int. J. Geomech.*, American Society of Civil Engineers, **3(1)**, 99-110. https://doi.org/10.1061/(ASCE)1532-3641(2003)3:1(99).

Jiang, N., Wang, C., Wu, Q. and Li, S. (2020), "Influence of structure and liquid limit on the secondary compressibility of soft soils", *J. Mar. Sci. Eng.*, **8**(9), 627. https://doi.org/10.3390/jmse8090627.

Kabbaj, M., Oka, F., Leroueil, S. and Tavenas, F. (1986), "Consolidation of natural clays and laboratory testing", *Consolid. Soils: Test. Eval.*, 378-404. https://doi.org/10.1520/STP34624S.

Kaczmarek, Ł. and Dobak, P. (2017), "Contemporary overview of soil creep phenomenon", *Contemp. Trend. Geosci.*, **6**(1), 28-40. https://doi.org/10.1515/ctg-2017-0003.

Kaniraj, S.R. and Gayathri, V. (2004), "Permeability and consolidation characteristics of compacted fly ash", *J. Energy Eng.*, **130**(1), 18-43. https://doi.org/10.1061/(ASCE)0733-9402(2004)130:1(18).

Kelln, C., Sharma, J., Hughes, D. and Graham, J. (2008), "An improved elastic–viscoplastic soil model", *Can. Geotech. J.*, **45**(10), 1356-1376. https://doi.org/10.1139/T08-057.

Khademi, F., and Budiman, J. (2016). "Expansive soil: causes and treatments", *i-Manager's J. Civil Eng.*, **6**(3), 1-13. https://doi.org/10.26634/jce.6.3.8083.

Leroueil, S., Kabbaj, M. and Tavenas, F. (1985), "Stress-strain-strain rate relation for the compressibility of sensitive natural clays", *Geotechnique*, **35**(2), 159-180. https://doi.org/10.1680/geot.1985.35.2.159.

Mesri, G. (1973), "Coefficient of secondary compression", *ASCE J. Soil Mech. Found. Div*., **99**, 123-137.

Mesri, G. and Castro, A. (1987), "C α/C c concept and K 0 during secondary compression", *J. Geotech. Eng.*, **113**(3), 230-247. https://doi.org/10.1061/(ASCE)0733-9410(1987)113:3(230).

Mesri, G. and Godlewski, P.M. (1977), "Time and stress-compressibility interrelationship", *ASCE J. Geotech. Eng. Div.*, **103**(5), 417-430. https://doi.org/10.1016/0148-9062(77)91005-1.

Mitchell, J.K. and Soga, K. (1993), *Fundamentals of Soil Behavior*, Wiley, New York.

Nash, D. (2001), "Modelling the effects of Surcharge to reduce long term settlement of reclamations over soft clays: A numerical Case Study", *Soil. Found., (Japanese Geotechnical Society)*, **41**(5), 1-13. https://doi.org/10.3208/sandf.41.5_1.

Navarro, A. (2001), "Secondary compression of clays as a local dehydration process", *Géotechnique*, **51**(10), 859-869. https://doi.org/10.1680/geot.2001.51.10.859.

Nelson, J.D. (2016), "Time dependence of swelling in oedometer tests on expansive soil", *Japanese Geotechnical Society Special Publication*, **2**(12), 490-493. https://doi.org/10.3208/jgssp.OTH-35.

Nelson, J.D., Chao, K.C., Overton, D.D. and Nelson, E.J. (2015), *Foundation engineering for expansive soils*, John Wiley & Sons.

Nowamooz, H. (2014), "Effective stress concept on multi-scale swelling soils", *Appl. Clay Sci.*, **101**, 205-214. https://doi.org/10.1016/j.clay.2014.07.036.

Powell, J.S., Take, W.A., Siemens, G. and Remenda, V.H. (2012), "Time-dependent behaviour of the Bearpaw Shale in oedometric loading and unloading", *Can.Geotech. J.*, **49**(4), 427-441. https://doi.org/10.1139/t2012-004.

Schofield, A. and Wroth, P. (1968), *Critical state soil mechanics*. McGraw-hill.

Shi, X.S., Yin, J., Feng, W. and Chen, W. (2018), "Creep coefficient of binary sand–bentonite mixtures in oedometer testing using mixture theory", *Int. J. Geomech.*, **18**(12), 4018159. https://doi.org/10.1061/(ASCE)GM.1943-5622.0001295.

Singh, M.J., Feng, W., Dong-Sheng, X. and Lalit, B. (2020), "Experimental sudy of compression behavior of Indian black cotton soil in oedometer condition", *Int. J. Geosynth. Ground Eng.*, **6**(2), 30. https://doi.org/10.1007/s40891-020-00207-0.

Sun, J. (1999). "Rheology of geomaterials and applications", *China Construction Publication House, Beijing, China*.

Tan, F., Zhou, W.H. and Yuen, K.V. (2018), "Effect of loading duration on uncertainty in creep analysis of clay", I*nt. J. Numer. Anal. Method. Geomech*., **42**(11), 1235-1254. https://doi.org/10.1002/nag.2788.

Terzaghi, K., Peck, R.B. and Mesri, G. (1996), *Soil mechanics in engineering practice*. John Wiley & Sons.

Villar, M.V. and Lloret, A. (2008), "Influence of dry density and water content on the swelling of a compacted bentonite", *Appl. Clay Sci.*, **39**(1-2), 38-49. https://doi.org/10.1016/j.clay.2007.04.007.

Wang, W., Luo, Q., Yuan, B. andn Chen, X. (2020), "An investigation of time-dependent deformation characteristics of soft dredger fill", *Adv. Civil Eng.*, **2020.** https://doi.org/10.1155/2020/8861260.

Yin, J.H. (1990), "Constitutive modelling of time-dependent stress-strain behaviour of soils", Ph.D. thesis, University of Manitoba, Winnipeg, March.

Yin J.H. and Graham, J. (1994), "Equivalent times and one-dimensional elastic viscoplastic modelling of time-dependent stress strain behavior of clays", *Can. Geotech. J.*, **31**, 42-52. https://doi.org/10.1139/t94-005.

Yin, J.H. (1999), "Non-linear creep of soils in oedometer tests", *Geotechnique*, **49**(5), 699-707. https://doi.org/10.1680/geot.1999.49.5.699.

Yin, J.H., Zhu, J.G. and Graham, J. (2002), "A new elastic viscoplastic model for time-dependent behaviour of normally and overconsolidated clays: theory and verification", *Can. Geotech. J.*, **39**(1), 157-173. https://doi.org/10.1139/t01-074.

Yin, J.H. and Tong, F. (2011), "Constitutive modeling of time-dependent stress–strain behaviour of saturated soils exhibiting both creep and swelling", *Can. Geotech. J.*, **48**(12), 1870-1885. https://doi.org/10.1139/t11-076.

Yin, J. (2013), "Review of Elastic Visco-Plastic Modeling of the Time-Dependent Stress-Strain Behavior of soils and its extension and applications", *Springer-Verlag Berlin Heidelberg*, (3), 149-157. https://doi.org/10.1007/978-3-642-32814-5_17.

Yin, J.H. (2015), "Fundamental issues of elastic viscoplastic modeling of the time-dependent stress–strain behavior of geomaterials", *Int. J. Geomech.*, **15**(5), https://doi.org/10.1061/(ASCE)GM.1943-5622.0000485.

Yuan, Y. (2016), "A new elasto-viscoplastic model for rate-dependent behavior of clays", Ph. D. Thesis, Massachusetts Institute of Technology.

Yuan, Y. and Whittle, A.J. (2018), "A novel elasto-viscoplastic formulation for compression behaviour of clays", *Géotechnique*, **68**(12), 1044-1055. https://doi.org/10.1680/jgeot.16.P.276.

Zdravkovic, L. and Carter, J. (2008), "Contributions to Géotechnique 1948-2008: Constitutive and numerical modelling", *Géotechnique*, **58**(5), 405-412. https://doi.org/10.1680/geot.2008.58.5.405.

Zhu, H.H., Zhang, C.C., Mei, G.X., Shi, B. and Gao, L. (2017), "Prediction of one-dimensional compression behavior of Nansha clay using fractional derivatives", *Mar. Georesour. Geotec.*, **35**(5), 688-697. https://doi.org/10.1080/1064119X.2016.1217958.

IC